JOE

Journal of Endodontics

March 2015 Volume 41, Number 3 www.jendodon.com

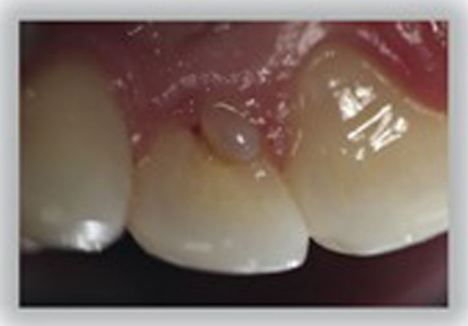

Unilateral Fusion of a Supernumerary Tooth to a Lateral Incisor Page 420

Official Journal of the American Association of Endodontists

ST2 Deletion Increases Inflammatory Bone Destruction in Experimentally Induced Periapical Lesions in Mice

Milena Velickovic, DDS, Nada Pejnovic, MD, PhD,* Slobodanka Mitrovic, MD, PhD,* Gordana Radosavljevic, MD, PhD,* Ivan Jovanovic, MD, PhD,* Tatjana Kanjevac, DDS, PhD,† Nemanja Jovicic, MD,* and Aleksandra Lukic, DDS, PhD‡*

Abstract

Introduction: ST2 is a member of the interleukin (IL)-1 receptor family, and IL-33 is its natural ligand. ST2 signaling promotes Th2 immune response in allergy, autoimmunity, and chronic inflammatory disorders, but its role in the pathogenesis of periapical lesions is unknown. The purpose of this study was to investigate whether ST2 gene deletion affects the development of experimentally induced periapical lesions in mice. **Methods:** Pulps of mandibular molars from wild-type (WT) and ST2 knockout ($ST2^{-/-}$) BALB/c mice were exposed and left open to the oral environment. After death, hemi-mandibles were isolated and prepared for histologic, immunohistochemical, and flow cytometric analysis. **Results:** The expression of IL-33 and its receptor ST2 was higher in periapical lesions in WT mice compared with normal root apices (both $P < .05$). The increased periapical bone loss observed in $ST2^{-/-}$ mice was associated with enhanced influx of neutrophils, CD3+ CXCR3+ Th1 cells, and CD3+ CCR6+ Th17 cells and increased number of tartrate-resistant acid phosphatase+ osteoclasts (all $P < .05$). Furthermore, periapical lesions in $ST2^{-/-}$ mice contained increased percentages of T cells expressing interferon-γ, IL-17, tumor necrosis factor-α, and IL-6 (all $P < .05$). In comparison with WT mice, CD3+ receptor activator of nuclear factor kappa B ligand+ T cells were increased, whereas CD3+ osteoprotegerin+ T cells were decreased in the lesions of $ST2^{-/-}$ mice (both $P < .05$). **Conclusions:** ST2 deletion increases inflammatory bone loss in experimental periapical lesions in mice, which is associated with enhanced Th1/Th17 cell mediated periapical immune responses and increased osteoclastogenesis. *(J Endod 2015;41:369–375)*

Key Words

Bone loss, inflammation, osteoclasts, periapical lesions, RANKL, ST2, Th1/Th17 cells

From the *Center for Molecular Medicine, Kragujevac, Serbia; †Department of Preventive and Pediatric Dentistry, Faculty of Medical Sciences, University of Kragujevac, Kragujevac, Serbia; and ‡Department of Endodontics, Faculty of Medical Sciences, University of Kragujevac, Kragujevac, Serbia.

Address requests for reprints to Dr Aleksandra Lukic, Faculty of Medical Sciences, University of Kragujevac, Svetozara Markovica 69, 34000 Kragujevac, Serbia. E-mail address: miodrag.lukic@medf.kg.ac.rs

0099-2399/$ - see front matter

http://dx.doi.org/10.1016/j.joen.2014.11.017

Periapical lesions develop in response to chronic stimulation caused by microorganisms that invade and destroy the dental pulp (1). The host's response appears to be similar to the response to bacterial infections elsewhere in the body, with the additional feature of the resorption of alveolar bone that surrounds the dental root apex (2). Osteoclasts are multinuclear tartrate-resistant acid phosphatase (TRAP) positive cells that are principally responsible for bone resorption, which differentiation and maturation are regulated by the balance between the receptor activator of nuclear factor kappa B ligand (RANKL) and its soluble decoy receptor osteoprotegerin (OPG) (3, 4). Th1- and Th17-derived cytokines together with interleukin (IL)-1, IL-6, and tumor necrosis factor (TNF)-α promote chronic inflammation and bone resorption, whereas Th2-derived cytokines and T-regulatory cells (Tregs) are responsible for the healing processes (5–11).

The ST2 gene, a member of the IL-1 receptor family (IL-1R), encodes a shorter soluble form and a transmembrane full-length form, sST2 and ST2L, respectively (12). ST2L is stable and selective marker of Th2 cells (13). Natural ligand for ST2L is IL-33, which is released on necrotic cell death during infection and inflammation. IL-33 is mainly expressed in the nucleus of fibroblasts and endothelial and epithelial cells (14) and potently enhances Th2 immune response (15). IL-33/ST2 signaling has a protective role in Th1/Th17 cell mediated inflammatory diseases such as experimental autoimmune encephalomyelitis, fulminant hepatitis, and type 1 diabetes (16–18).

The aim of this study was to investigate whether the lack of ST2 signaling affects inflammatory bone destruction in experimentally induced periapical lesions in mice.

Materials and Methods

Mice

IL-33 receptor knockout mice ($ST2^{-/-}$ mice) on the BALB/c background were generated by a targeted disruption of mouse ST2 gene (19). $ST2^{-/-}$ mice were provided by Dr McKenzie (University of Cambridge, United Kingdom). We used 6- to 8-week-old male wild-type (WT) and $ST2^{-/-}$ mice for the induction of periapical lesions. All animals were maintained in our animal facilities under standard laboratory conditions and received humane care. Experiments were approved by the Animal Ethics Committee of the Faculty of Medical Sciences, University of Kragujevac, Serbia.

Induction of Periapical Lesions

Mice were anesthetized with ketamine hydrochloride (60 mg/kg body weight) and xylazine (10 mg/kg body weight) by intraperitoneal injection. Mandibular molar pulps were exposed by using a high-speed electric dental handpiece (W&H Dentalwerk, Burmoos, Austria) (20). For histologic, morphometric, and immunohistochemical analyses, periapical lesions were induced by pulp exposure of the mandibular first molar pulps. For flow cytometric analysis, mice were subjected to both first and second mandibular molar pulp exposure. Mice were killed 14 and 28 days after lesion induction.

Immunohistochemistry

Paraffin-embedded sections of periapical lesions and normal root apices from WT mice were deparaffinized and incubated with primary rabbit anti-IL-33 antibody (sc-98660; Santa Cruz Biotechnology, Santa Cruz, CA; 1:100), followed by visualization by using Expose Rb specific HRP/DAB detection IHC kit (Abcam, Cambridge, UK).

Tissue sections were incubated with rabbit polyclonal anti-ST2 antibody (PA5-20077; Thermo Fisher Scientific, Waltham, MA; 1:500) and visualized by using Expose Rb specific HRP/AEC detection IHC kit (Abcam). Sections were counterstained with hematoxylin, and counts of positive cells were determined by using Image J 1.36 software (National Institutes of Health, Bethesda, MD).

Sections of periapical lesions from ST2$^{-/-}$ and WT mice were incubated with primary goat anti-TRAP antibody (sc-30833; Santa Cruz Biotechnology; 1:100) followed by incubation with biotinylated secondary donkey anti-goat antibody (sc-2042) and visualized by using Expose Rb specific HRP/DAB detection IHC kit. For each specimen, multinucleated TRAP-positive cells in the periapical tissues in 5 randomly selected areas were counted by using $\times$400 magnification, and the average numbers of positive cells per high-power field were determined.

Histologic and Morphometric Analysis

Hemi-mandibles were isolated and fixed in 4% paraformaldehyde in phosphate-buffered saline, decalcified in 3% formic acid, and embedded in paraffin. Tissue blocks were cut in longitudinal serial sections of 4-μm thickness and stained with hematoxylin-eosin.

Sections that included the distal root of the mandibular first molar and passing through the apical foramen or close to it were selected for morphometric analysis. The sections were photographed with a digital camera mounted on light microscope (Olympus BX51, Tokyo, Japan), and the bone resorption area and neutrophil count were determined by using the Image J 1.36 software. The area of the lesion was traced surrounding the apical third of the root. The extent of the resorption areas was obtained by analysis of the minimum of 3 sections per tooth. The values of lesion sizes, in square millimeters, were averaged to obtain summary measures of bone resorption for each animal. Then the neutrophils were counted and expressed as a number per square millimeter of lesion area.

Isolation of Periapical Lesion and Cervical Lymph Node Cells

Hemi-mandibles were isolated, and the periapical tissues surrounding the roots of the lower first and second molars were carefully extracted with the surrounding bone as block specimens, as previously described (21). The isolated bone blocks then were treated with RPMI-1640 medium containing 1 mg/mL collagenase type IV (Life Technologies, Carlsbad, CA) and 1 mmol/L EDTA for 60 minutes at 37°C, forced gently through cell strainer (BD Pharmingen, San Diego, CA), and resuspended in RPMI-1640 medium.

Cervical lymph nodes were isolated, forced gently through cell strainer, and resuspended in RPMI-1640 medium containing 10% fetal bovine serum.

Flow Cytometry

Cervical lymph node and periapical tissue cell suspensions were incubated with fluorochrome-labeled antibodies specific for CD3, CD4, CD8, CXCR3, CCR6, CD11c, CD11b, F4/80, CD49b (BD Pharmingen), and RANKL (Santa Cruz Biotechnology) or isotype-matched controls (BD Pharmingen). For intracellular staining, cells were activated with PMA (50 ng/mL)/ionomycin (500 ng/mL) (Sigma-Aldrich, St Louis, MO) with Golgy Stop (BD Pharmingen) for 4 hours and processed (22). Fluorochrome-labeled antibodies specific for TNF-α, IL-6, interferon (IFN)-γ, IL-17, IL-4, IL-5 (BD Pharmingen), and OPG (Santa Cruz Biotechnology) were used. Intracellular staining for Foxp3 was performed by using the BD Bioscience fixation/permeabilization buffer kit.

Fluorescence-activated cell sorter analysis was done by using FACSCalibur (BD), and the results were analyzed with Flowing Software Version 2.5 (Informer Technologies, Dominica).

Statistical Analysis

The data were analyzed by using statistical package SPSS (SPSS Inc, Chicago, IL), version13. Descriptive statistics including the mean and standard error were calculated. Comparisons between groups were performed by using Mann-Whitney rank sum test. The results were considered significantly different when $P < .05$.

Results

Expression of IL-33 and ST2 in Periapical Tissue

The number of IL-33$^+$ cells was significantly higher in periapical lesions (Fig. 1*A*, *upper panel*) compared with normal root apices (Fig. 1*A*, *lower panel*) (235 $\pm$ 12 cells/mm^2 versus 121 $\pm$ 7 cells/mm^2, $P < .05$, Fig. 1*B*). Similarly, the number of ST2$^+$ cells was significantly higher in periapical lesions (Fig. 1*C*, *upper panel*) compared with normal root apices (Fig. 1*C*, *lower panel*) (152 $\pm$ 16 cells/mm^2 versus 53 $\pm$ 4 cells/mm^2, $P < .05$, Fig. 1*D*).

ST2 Deletion Increases Severity of Periapical Lesions

At days 14 and 28 after pulp exposure, inflammatory cell infiltration and the alveolar bone resorption in the periapical tissue were more pronounced in ST2$^{-/-}$ mice compared with WT mice (Fig. 2*A* and *B*).

The lesions in ST2$^{-/-}$ mice were significantly larger compared with WT mice ($P < .05$, Fig. 2*C*), and the neutrophil count per square millimeter of lesion area in ST2$^{-/-}$ mice was significantly higher than in WT mice at both experimental periods ($P < .05$, Fig. 2*D*).

ST2 Deletion Favors Th1/Th17 Response in Periapical Lesions and Cervical Lymph Nodes

The numbers of mononuclear cells (MNCs) in the periapical lesions and cervical lymph nodes were significantly higher in ST2$^{-/-}$ mice compared with WT mice at 14 and 28 days after lesion induction (both $P < .05$, Fig. 3).

Periapical lesions of ST2$^{-/-}$ mice had increased percentages of CD4$^+$ T cells and CXCR3$^+$ and CCR6$^+$ cells among gated CD3$^+$ T cells at both experimental time points ($P < .05$, Fig. 3). The percentages of CD11c$^+$ dendritic cells (DCs), CD11b$^+$ myeloid cells, F4/80$^+$ macrophages, CD49b$^+$ natural killer (NK) cells, CD49b$^+$ CD3$^+$ natural killer T (NKT)-like cells, CD8$^+$ T cells, and CD4+ FoxP3+ Tregs did not differ between lesions of ST2$^{-/-}$ and WT mice 14 days after pulp exposure (data not shown).

The percentages of gated CD4$^+$ cells expressing TNF-α, IL-6, IFN-γ, and IL-17 in periapical lesions were significantly higher in ST2$^{-/-}$ compared with WT mice 14 days after pulp exposure ($P < .05$, Fig. 3*A*), with no difference in the percentages of IL-4$^+$ and IL-5$^+$ cells (data not shown). The percentages of gated CD4$^+$ cells expressing IFN-γ and IL-17 and gated CD3$^+$ cells expressing RANKL in periapical lesions were significantly higher in ST2$^{-/-}$ compared with WT mice 28 days after lesion induction. However, the percentages of gated CD3$^+$ cells expressing OPG in periapical lesions were significantly higher in WT mice ($P < .05$, Fig. 3*B*).

There were significantly higher percentages of CD11c$^+$ DCs, CD11b$^+$ myeloid cells, CXCR3$^+$ Th1 cells, and CCR6$^+$ Th17 cells among gated CD3$^+$ T cells in the cervical lymph nodes of ST2$^{-/-}$ mice compared with WT mice 14 days after pulp exposure ($P < .05$, Fig. 3*A*). There was no difference in the percentages of F4/80$^+$ macrophages, CD49b$^+$ NK cells, CD49b$^+$ CD3$^+$ NKT-like cells, CD4$^+$ T cells, CD8$^+$ T cells, and CD4$^+$ FoxP3$^+$ Tregs, as well as CD4$^+$ cells expressing TNF-α, IL-6, IFN-γ, IL-17, IL-4, and IL-5 at day 14 after lesion induction (data not shown).

The percentages of gated CD3$^+$ cells expressing CXCR3, CCR6, and RANKL in lymph nodes were significantly higher in ST2$^{-/-}$ compared

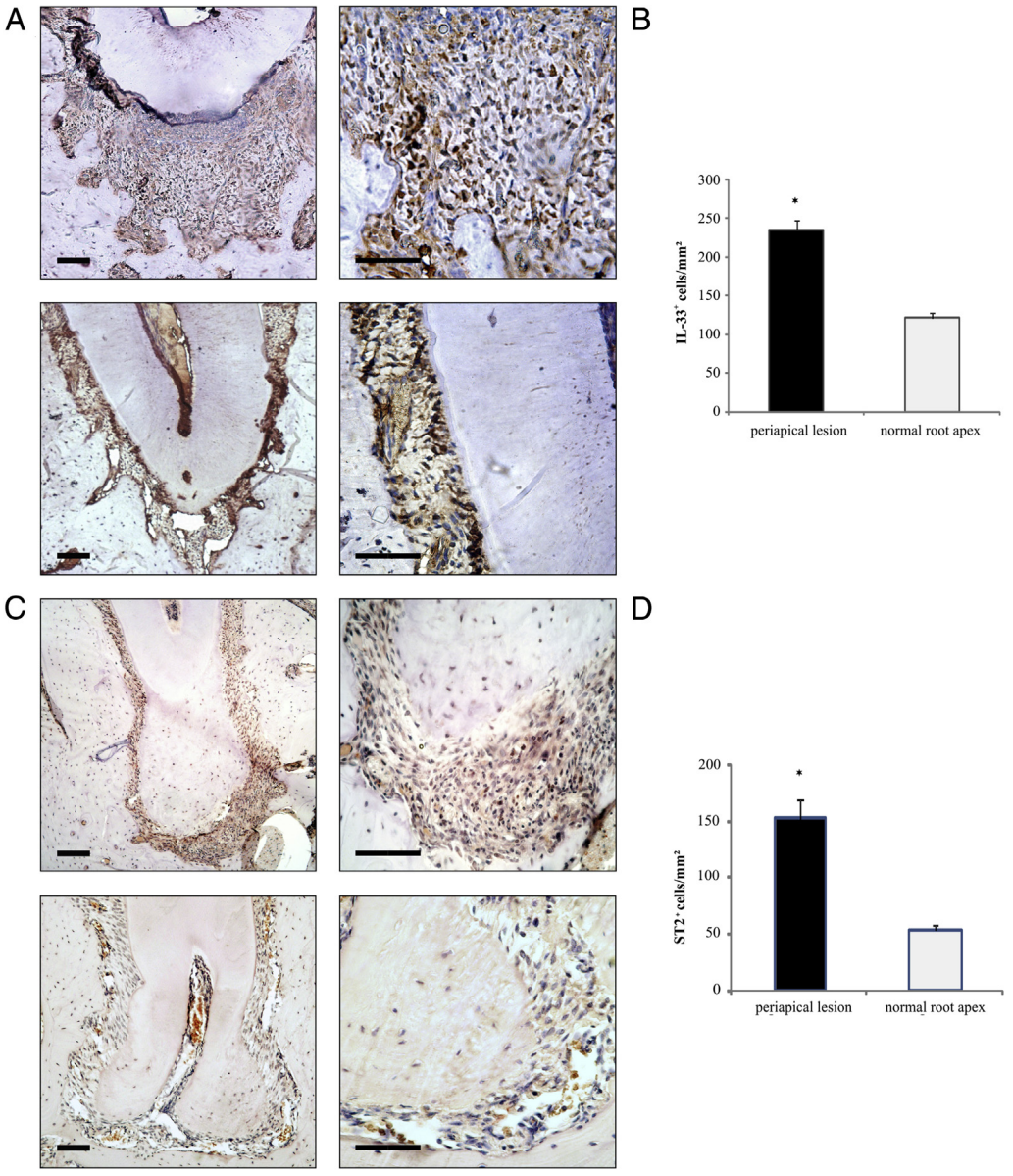

Figure 1. IL-33 and ST2 expression in periapical tissues. (*A*) Photomicrographs of representative IL-33 positive staining in periapical lesions ($n = 6$) and normal root apices from wild-type BALB/c mice ($n = 6$). Brown-colored cells indicate IL-33–positive cells. Photomicrographs show increased expression of IL-33 in periapical lesion (*upper panel*) compared with normal root apex (*lower panel*). (*B*) The number of IL-33–positive cells was significantly higher in periapical lesions compared with normal root apices (mean ± standard error of the mean, $^*P < .05$). (*C*) Photomicrographs of representative ST2 positive staining in periapical lesions ($n = 6$) and normal root apices from wild-type BALB/c mice ($n = 6$). Brown-colored cells indicate ST2 positive cells. Photomicrographs show increased expression of ST2 in periapical lesion (*upper panel*) compared with normal root apex (*lower panel*). Original magnification, ×100 (*left,* scale bar = 100 μm) and ×400 (*right,* scale bar = 50 μm). (*D*) The number of ST2 positive cells was significantly higher in periapical lesions compared with normal root apices (mean ± standard error of the mean, $^*P < .05$).

with WT mice, whereas the percentages of gated $CD3^+$ cells expressing OPG were significantly higher in WT mice 28 days after pulp exposure ($P < .05$, Fig. 3*B*). There was no difference in the percentages of gated $CD4^+$ cells expressing IFN-γ and IL-17 (data not shown).

ST2 Deletion Increases Number of $TRAP^+$ Osteoclasts in Periapical Tissue

Determination of $TRAP^+$ osteoclasts on bone periphery adjacent to periapical lesions showed significantly higher number of $TRAP^+$ multinucleated cells in $ST2^{-/-}$ mice when compared with WT mice (6.8 ± 0.9 osteoclasts/high-power field versus 4.1 ± 0.4 osteoclasts/high-power field, $P < .05$, Fig. 4*A*). We evaluated the total numbers of $RANKL^+$ and OPG^+ MNCs in the lesions determined by flow cytometry, and RANKL/OPG ratio was significantly increased in $ST2^{-/-}$ mice compared with WT mice (Fig. 4*C*).

Discussion

Here we provided the first evidence that ST2 signaling plays an important role in the pathogenesis of periapical lesions. First, we demonstrated the increased expression of IL-33 and ST2 in murine

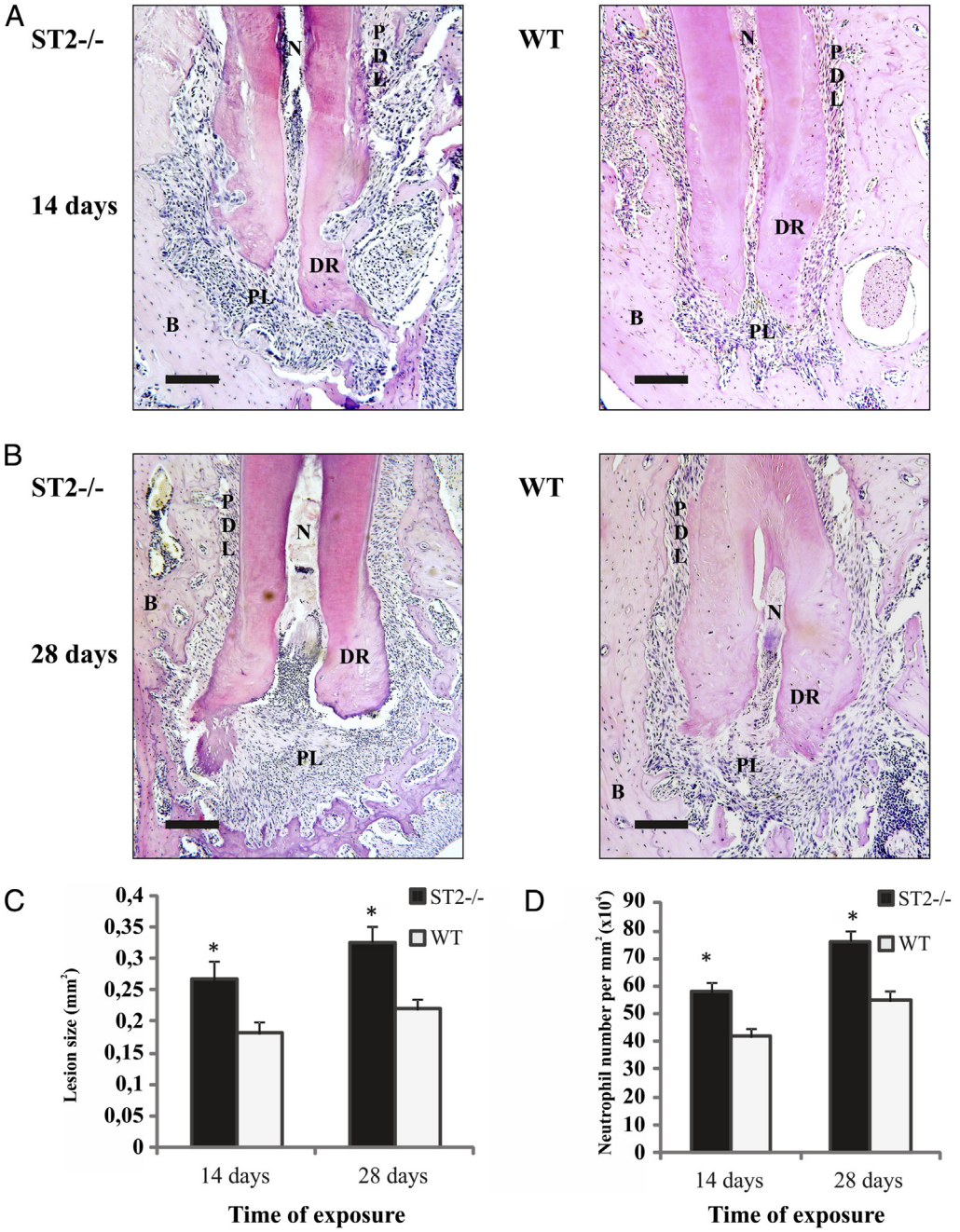

Figure 2. Effect of pulp exposure of mandibular first molars to oral pathogens in ST2$^{-/-}$ and WT mice. (*A*) Photomicrograph of representative hematoxylin-eosin stained periapical lesions in ST2$^{-/-}$ and WT mice 14 days after pulp exposure of mandibular first molars. (*B*) Photomicrograph of representative hematoxylin-eosin stained periapical lesions in ST2$^{-/-}$ and WT mice 28 days after pulp exposure of mandibular first molars. B, bone; DR, distal root of mandibular first molar; N, necrosis of pulpal tissue; PDL, periodontal ligament; PL, periapical lesion. Original magnification, ×100; scale bar = 100 μm. (*C* and *D*) Kinetics of periapical lesion formation after pulp exposure in ST2$^{-/-}$ and WT mice. ST2$^{-/-}$ and WT mice were killed at days 14 (n = 8/group) and 28 (n = 8/group) after induction of periapical lesions. The differences between lesion sizes (*C*) and neutrophil count in the periapical region (*D*) between ST2$^{-/-}$ and WT mice were significantly different at 14 and 28 days after pulp exposure (mean ± standard error of the mean, *P < .05).

periapical lesions of WT BALB/c mice (Fig. 1). Furthermore, we showed that targeted disruption of ST2 gene in BALB/c mice led to enhanced periapical destruction (Fig. 2), which was associated with increased number of TRAP^{+} osteoclasts (Fig. 4) and massive infiltration of immune effector cells expressing proinflammatory cytokines (Fig. 3).

The increased expression of IL-33 and ST2 in periapical lesions in WT mice (Fig. 1) indicates their involvement in the pathogenesis of periapical lesions. Recent study showed that IL-33 produced by osteoblasts inhibits osteoclastogenesis through ST2 and that mice lacking ST2 gene displayed low bone mass caused by increased osteoclastogenesis (23). The present study showed that deletion of ST2 signaling augmented the RANKL/OPG ratio in periapical lesions (Fig. 4*C*) and dependently increased the number of TRAP-positive osteoclasts (Fig. 4*B*) and periapical bone resorption (Fig. 2*C*).

In addition, we demonstrated that ST2 gene ablation significantly enhanced influx of neutrophils (Fig. 2*D*). This finding is in agreement

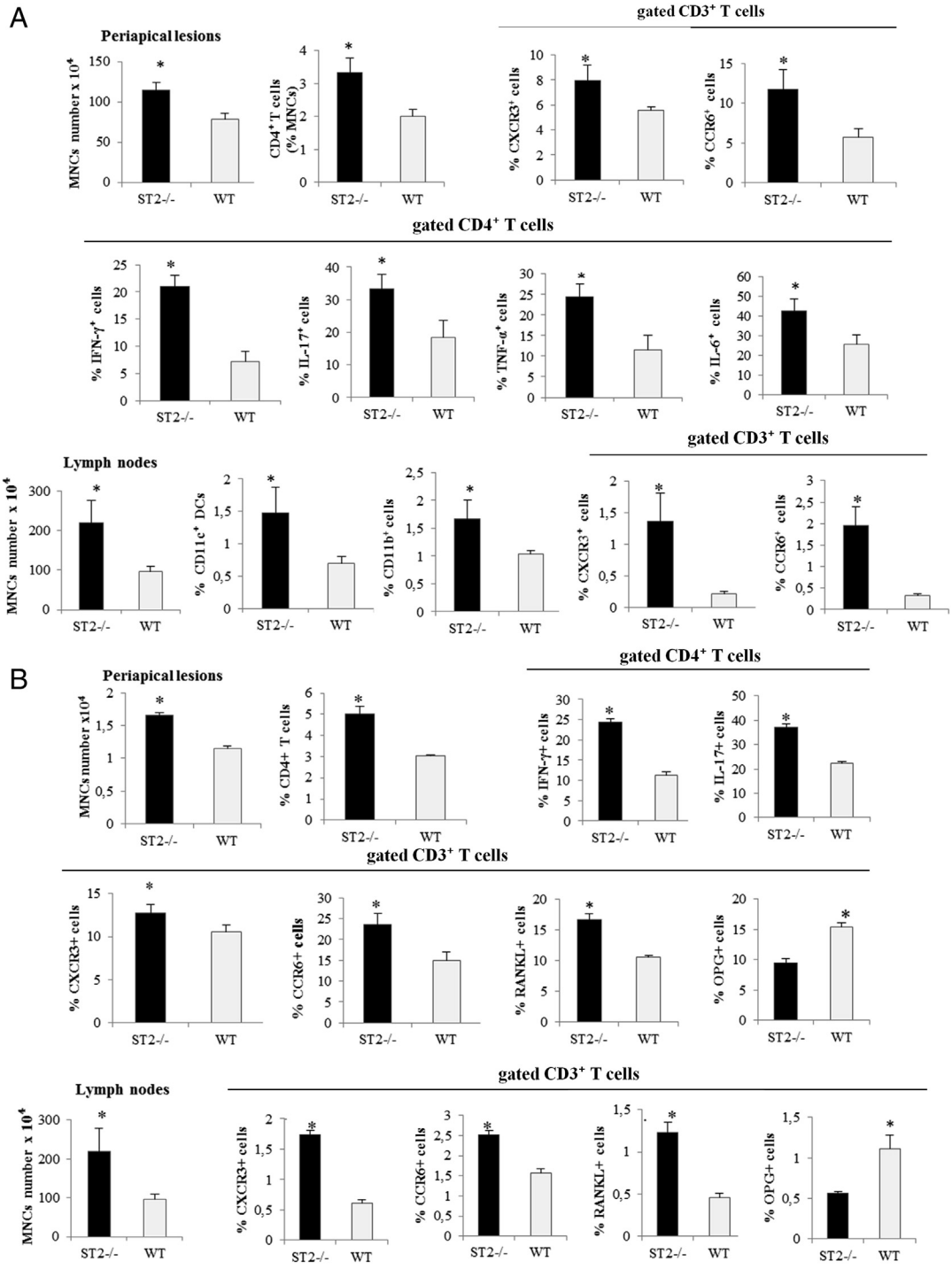

Figure 3. Flow cytometric analyses of cervical lymph node and periapical lesion MNCs 14 days (*A*) and 28 days after lesion induction (*B*). Analyses of cervical lymph node and periapical lesion MNCs were done by first gating the MNCs by size and granularity on forward scatter (FSC)/side scatter (SSC). Then $CD3^+$ or $CD4^+$ cells were gated, and percentages of TNF-α, IL-6, IFN-γ, IL-17, etc among gated cells were determined. (*A*) Total MNC number was significantly higher in periapical lesions of $ST2^{-/-}$ mice ($n = 8$) compared with WT mice ($n = 8$). Percentages of $CD4^+$ T cells and $CXCR3^+$ and $CCR6^+$ cells in gated $CD3^+$ T cells as well as TNF-α^+, IL-6^+, IFN-γ^+, and IL-17^+ cells among gated $CD4^+$ T cells were significantly higher in $ST2^{-/-}$ mice compared with WT mice. Total MNC number was significantly higher in cervical lymph nodes of $ST2^{-/-}$ mice compared with WT mice. Significantly higher percentages of $CD11c^+$ DCs, $CD11b^+$ myeloid cells, as well as $CXCR3^+$ and $CCR6^+$ cells in gated $CD3^+$ T cells were noticed in cervical lymph nodes of $ST2^{-/-}$ mice compared with WT controls (mean $\pm$ standard error of the mean, $^*P <$ .05). (*B*) Total MNC number was significantly higher in periapical lesions of $ST2^{-/-}$ mice ($n = 8$) compared with WT mice ($n = 8$). Percentages of $CD4^+$ T cells, IFN-γ^+, and IL-17^+ cells among gated $CD4^+$ T cells and $CXCR3^+$, $CCR6^+$, and $RANKL^+$ cells in gated $CD3^+$ T cells were significantly higher in $ST2^{-/-}$ mice compared with WT mice, whereas OPG^+ cells in gated $CD3^+$ T cells were significantly higher in WT mice. Total MNC number was significantly higher in cervical lymph nodes of $ST2^{-/-}$ mice compared with WT mice. Significantly higher percentages of $CXCR3^+$, $CCR6^+$, and $RANKL^+$ cells in gated $CD3^+$ T cells were noticed in cervical lymph nodes of $ST2^{-/-}$ mice compared with WT mice, whereas percentages of OPG^+ cells in gated $CD3^+$ T cells were significantly higher in WT controls (mean $\pm$ standard error of the mean, $^*P < .05$).

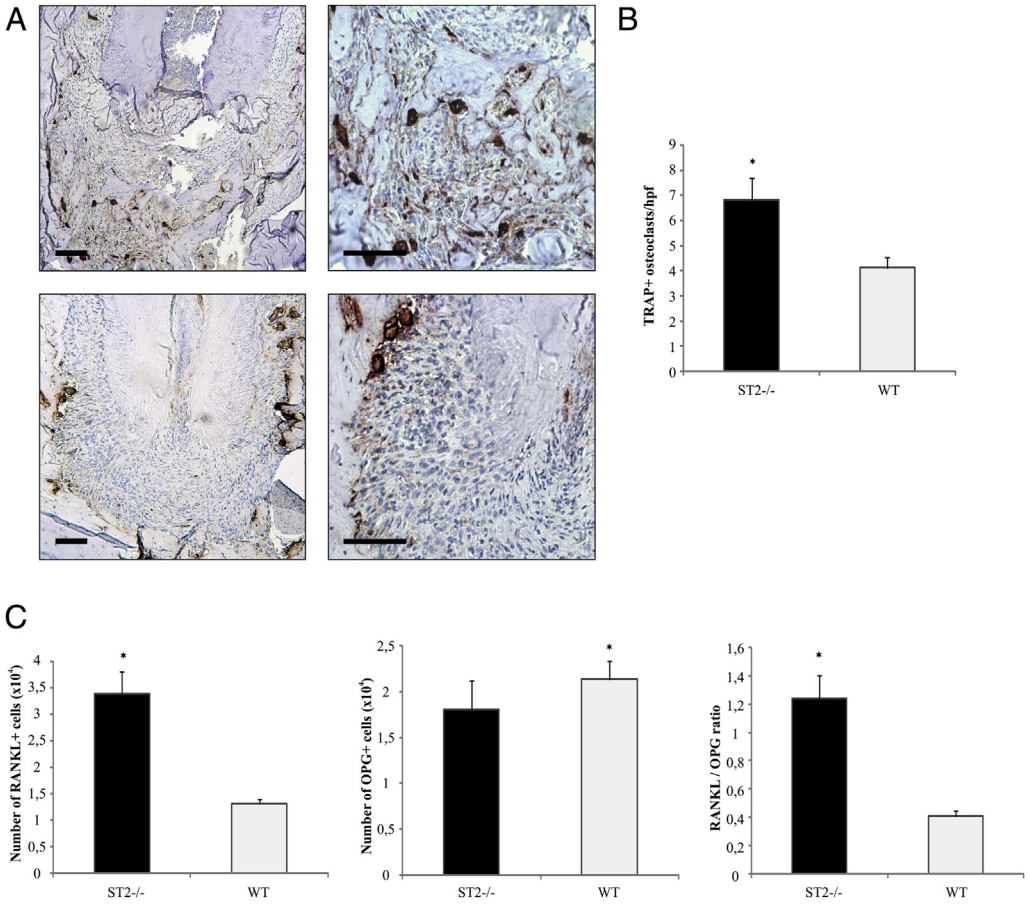

Figure 4. TRAP-positive multinucleated cells, total number of RANKL-positive and OPG-positive cells, and RANKL/OPG ratio in periapical tissue. (*A*) Photomicrographs of representative TRAP-positive staining in periapical lesions of ST2$^{-/-}$ (n = 6) and WT BALB/c mice (n = 6). Brown-colored cells indicate TRAP-positive multinucleated osteoclasts. (*B*) Photomicrographs show markedly increased number of osteoclasts in periapical lesions of ST2$^{-/-}$ mice (*upper panel*) compared with WT mice (*lower panel*) (mean ± standard error of the mean, *P < .05). Original magnification, ×100 (left, scale bar = 100 μm) and ×400 (right, scale bar = 50 μm). (*C*) Total number of RANKL-positive MNCs was significantly higher in periapical lesions of ST2$^{-/-}$ mice compared with WT mice 28 days after pulp exposure, whereas total number of OPG-positive cells in periapical lesions was significantly higher in WT mice (mean ± standard error of the mean, *P < .05). Deletion of ST2 gene increased RANKL/OPG ratio in periapical lesions (mean ± standard error of the mean, *P < .05). hpf, high-power field.

with the results of Sakai et al (24) that IL-33 repressed neutrophil recruitment in liver ischemia/reperfusion model.

CD4$^+$ T cells predominate during active phase of lesion development (25, 26), and priming of naive T cells by DCs occurs in cervical lymph nodes in apical periodontitis. We found significantly higher percentages of CD11c$^+$ DCs in cervical lymph nodes and CD4$^+$ T cells in periapical tissues of ST2$^{-/-}$ mice compared with WT mice 14 days after lesion induction (Fig. 3*A*), which might indicate enhanced ability of DCs to stimulate proliferation of CD4$^+$ T cells in the absence of T1/ST2 gene (16).

TNF-α and IL-6 have bone resorptive effects in periapical lesion development (2, 25). We found significantly higher percentages of CD4$^+$ cells expressing TNF-α and IL-6 in periapical lesions of ST2$^{-/-}$ mice compared with WT mice during the active phase of periapical lesion expansion (Fig. 3*A*).

Th1 cells generally predominate in periapical lesions and potentiate inflammation and bone resorption (2,5–7). We demonstrated significantly higher number of CD4$^+$ IFN-γ^+ Th1 cells in periapical lesions of ST2$^{-/-}$ mice at both experimental periods (Fig. 3).

Th17 immune response plays a role in exacerbation of inflammation within periapical lesions (10, 27). We found significantly higher percentages of CD4$^+$ IL-17$^+$ Th17 cells in periapical lesions of ST2$^{-/-}$ mice compared with WT mice at both experimental periods (Fig. 3). These results are in accordance with previous findings that Th17 cells are associated with both active and chronic phase of periapical lesions (9).

In addition, significantly higher percentages of CD3$^+$ CXCR3$^+$ Th1 and CD3$^+$ CCR6$^+$ Th17 cells were found both at the site of infection and in draining lymph nodes of ST2$^{-/-}$ mice (Fig. 3). These chemokine receptors expressed on Th1 and Th17 cells, respectively, are involved in the migration of T cells to the inflamed tissues (28, 29).

Recent study has shown that RANKL produced by CD3$^+$ T lymphocytes contributes to osteoclast-mediated bone resorption in the periapical lesions (30). Indeed, we found significantly higher number of CD3$^+$ RANKL$^+$ cells (Fig. 3*B*), along with TRAP$^+$ osteoclasts (Fig. 4*B*), in periapical lesions of ST2$^{-/-}$ mice compared with WT mice 28 days after lesion induction, whereas the percentages of CD3$^+$ OPG$^+$ cells were significantly higher in WT mice (Fig. 3).

In conclusion, we provide the first evidence that deletion of ST2 signaling enhanced inflammatory bone destruction in experimentally induced periapical lesions in mice by promoting Th1/Th17 cell mediated immune response and osteoclastogenesis within the periapical lesions.

Acknowledgments

This study was supported by grants from the Serbian Ministry of Science and Technological Development (OP 175071), Serbia.

The authors deny any conflicts of interest related to this study.

References

1. Nair PN. Apical periodontitis: a dynamic encounter between root canal infection and host response. Periodontol 2000 1997;13:121–48.
2. Kawashima N, Stashenko P. Expression of bone-resorptive and regulatory cytokines in murine periapical inflammation. Arch Oral Biol 1999;44:55–66.
3. Teitelbaum SL. Bone resorption by osteoclasts. Science 2000;289:1504–8.
4. Belibasakis GN, Rechenberg DK, Zehnder M. The receptor activator of NF-κB ligand-osteoprotegerin system in pulpal and periapical disease. Int Endod J 2013;46:99–111.
5. Henriques LC, de Brito LC, Tavares WL, et al. Cytokine analysis in lesions refractory to endodontic treatment. J Endod 2011;37:1659–62.
6. de Brito LC, Teles FR, Teles RP, et al. T-lymphocyte and cytokine expression in human inflammatory periapical lesions. J Endod 2012;38:481–5.
7. de Carvalho Fraga CA, Alves LR, de Sousa AA, et al. Th1 and Th2-like protein balance in human inflammatory radicular cysts and periapical granulomas. J Endod 2013;39:453–5.
8. Colić M, Gazivoda D, Vucević D, et al. Proinflammatory and immunoregulatory mechanisms in periapical lesions. Mol Immunol 2009;47:101–13.
9. Yang S, Zhu L, Xiao L, et al. Imbalance of interleukin-17+ T-cell and Foxp3+ regulatory T-cell dynamics in rat periapical lesions. J Endod 2014;40:56–62.
10. Colić M, Vasilijić S, Gazivoda D, et al. Interleukin-17 plays a role in exacerbation of inflammation within chronic periapical lesions. Eur J Oral Sci 2007;115:315–20.
11. Colić M, Gazivoda D, Vucević D, et al. Regulatory T-cells in periapical lesions. J Dent Res 2009;88:997–1002.
12. Bergers G, Reikerstorfer A, Braselmann S, et al. Alternative promoter usage of the Fos-responsive gene Fit-1 generates mRNA isoforms coding for either secreted or membrane-bound proteins related to the IL-1 receptor. EMBO J 1994;13:1176–88.
13. Xu D, Chan WL, Leung BP, et al. Selective expression of a stable surface molecule on type 2 but not type 1 helper T cells. J Exp Med 1998;187:787–94.
14. Liew FY, Pitman NI, McInnes IB. Disease-associated function of IL-33: the new kid in the IL-1 family. Nat Rev Immunol 2010;10:103–10.
15. Schmitz J, Owyang A, Oldham E, et al. IL-33, an interleukin-1-like cytokine that signals via the IL-1 receptor-related protein ST2 and induces T helper type 2-associated cytokines. Immunity 2005;23:479–90.
16. Milovanovic M, Volarevic V, Ljujic B, et al. Deletion of IL-33R (ST2) abrogates resistance to EAE in BALB/c mice by enhancing polarization of APC to inflammatory phenotype. PLoS One 2012;7:e45225.
17. Volarevic V, Mitrovic M, Milovanovic M, et al. Protective role of IL-33/ST2 axis in Con A-induced hepatitis. J Hepatol 2012;56:26–33.
18. Zdravkovic N, Shahin A, Arsenijevic N, et al. Regulatory T cells and ST2 signaling control diabetes induction with multiple low doses of streptozotocin. Mol Immunol 2009;47:28–36.
19. Townsend MJ, Fallon PG, Matthews DJ, et al. T1/ST2-deficient mice demonstrate the importance of T1/ST2 in developing primary T helper cell type 2 responses. J Exp Med 2000;191:1069–76.
20. Yu SM, Stashenko P. Identification of inflammatory cells in developing rat periapical lesions. J Endod 1987;13:535–40.
21. AlShwaimi E, Purcell P, Kawai T, et al. Regulatory T cells in mouse periapical lesions. J Endod 2009;35:1229–33.
22. Pejnovic N, Pantic J, Jovanovic I, et al. Galektin-3 deficiency accelerates high-fat diet-induced obesity and amplifies inflammation in adipose tissue and pancreatic islets. Diabetes 2013;62:1932–44.
23. Schulze J, Bickert T, Beil FT, et al. Interleukin-33 is expressed in differentiated osteoblasts and blocks osteoclast formation from bone marrow precursor cells. J Bone Miner Res 2011;26:704–17.
24. Sakai N, Van Sweringen HL, Quillin RC, et al. Interleukin-33 is hepatoprotective during liver ischemia/reperfusion in mice. Hepatology 2012;56:1468–78.
25. Stashenko P, Wang CY. Characterization of bone resorptive mediators in active periapical lesions. Proc Finn Dent Soc 1992;88:427–32.
26. Kawashima N, Okiji T, Kosaka T, Suda H. Kinetics of macrophages and lymphoid cells during the development of experimentally induced periapical lesions in rat molars: a quantitative immunohistochemical study. J Endod 1996;22:311–6.
27. Fossiez F, Djossou O, Chomarat P, et al. T cell interleukin-17 induces stromal cells to produce proinflammatory and hematopoietic cytokines. J Exp Med 1996;183:2593–603.
28. Kabashima H, Yoneda M, Nagata K, et al. The presence of chemokine receptor (CCR5, CXCR3, CCR3)-positive cells and chemokine (MCP1, MIP-1alpha, MIP-1beta, IP-10)-positive cells in human periapical granulomas. Cytokine 2001;16:62–6.
29. Nakanishi T, Takahashi K, Hosokawa Y, et al. Expression of macrophage inflammatory protein 3alpha in human inflamed dental pulp tissue. J Endod 2005;31:84–7.
30. Silva MJ, Kajiya M, AlShwaimi E, et al. Bacteria-reactive immune response may induce RANKL-expressing T cells in the mouse periapical bone loss lesion. J Endod 2012;38:346–50.